Detection Performance of MIMO Unique Word OFDM

Victor Tomashevich and Ilia Polian
Faculty of Mathematics and Computer Science, University of Passau, Germany, Innstr. 41, 94032
Email: {victor.tomashevich, ilia.polian}@uni-passau.de

***Abstract*—This paper introduces generalization of unique word OFDM (orthogonal frequency division multiplexing) signaling scheme to multiple antennas (MIMO). As UW-OFDM represents a virtual massive MIMO system, the quasi-maximum likelihood (ML) detection algorithms initially introduced for massive MIMO systems are adapted to MIMO UW-OFDM. Results show that in an uncoded system MIMO UW-OFDM is able to exceed ML performance of MIMO CP-OFDM. However, the complexity penalty is not negligible. In case of a coded system, ML detected MIMO CP-OFDM still performs better. MIMO UW-OFDM represents a performance/complexity tradeoff between linear and ML detected MIMO CP-OFDM.**

I. Introduction

OFDM systems require insertion of a guard interval (GI) into the time domain data frame in order to combat inter-symbol interference caused by multipath propagation. Conventional OFDM systems use the cyclic prefix (CP), which is simply a copy of a data fraction, and is therefore random. On the contrary, UW-OFDM signaling uses a deterministic sequence in the GI, denoted as the unique word (UW) [1]. Frame structures of CP- and UW-OFDM are outlined in Fig. 1.

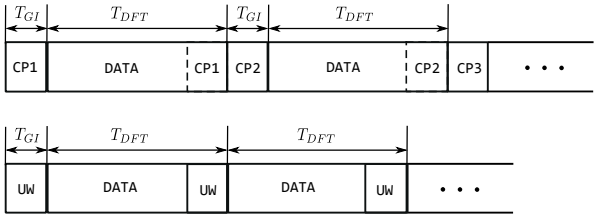

Fig. 1: UW vs CP frame structure

As UW is a known sequence, it can be used for synchronization or channel estimation purposes. The spectral efficiency of UW system remains unaffected. It can be observed from Fig. 1 that UW is the part of the Discrete Fourier Transform (DFT) interval, whereas CP is not. Therefore the length of the UW-OFDM frame is reduced from $T_{DFT} + T_{GI}$ to T_{DFT}, thus retaining the overall spectral efficiency [2].

More importantly, UW generation introduces a form of coding across sub-carriers [3]. UW can be generated by both systematic and non-systematic encoding [4].

The unique word signaling has been initially introduced for single-antenna systems (SISO). The inherent coding across sub-carriers allows much better BER performance compared to SISO CP-OFDM [2], [4]. Due to coding, the UW-OFDM system can also be viewed as a virtual MIMO system, where the size of the virtual channel matrix is given by the number of sub-carriers. Therefore, the MIMO maximum likelihood (ML) detection (Sphere decoding (SD)) have been applied [5]. However, the exponential complexity of SD restricted its use only to systems with low number of sub-carriers [5], [6].

UW-OFDM clearly outperforms CP-OFDM in SISO case [1], [2], [4]. However, current standards employ MIMO with M_t transmit and M_r receive physical antennas. This paper generalizes UW-OFDM scheme to a MIMO system and compares its performance against a MIMO CP-OFDM system. The employment of multiple antennas increases the system size further, and MIMO UW-OFDM can be regarded as a virtual massive MIMO system. It is therefore impossible to apply SD. Hence, it is resorted to quasi-ML algorithms initially introduced for massive MIMO systems. In this work, likelihood ascent search (LAS) algorithms [7], [8] are adapted to MIMO UW-OFDM because of their good performance and scalable complexity in very large MIMO systems.

To the best of the authors knowledge, this is the first analysis of MIMO UW-OFDM and its performance against MIMO CP-OFDM. The contributions of this paper are as follows. It is found that encoding the individual data streams (relative to transmit antennas) by distinct non-systematic UW generator matrices improves LAS BER performance. The soft output LAS does not perform well in a MIMO UW-OFDM coded system. Therefore, the LAS algorithm is modified to take into account the log likelihood ratios provided by its initial solution. The modified LAS and proposed soft output computation deliver better performance in a coded system than the original algorithm.

The rest of this paper is organized as follows. Section II introduces systematic and non-systematic generation of UWs [1], [4]. Sec. III discusses the generalization of UW signaling to a MIMO system with M_t transmit and M_r receive antennas. Section IV discusses linear and quasi-ML detection for MIMO UW-OFDM, Section V provides simulation results, and Section VI concludes the paper.

II. UW-OFDM

A. Systematic generation of UW

In UW-OFDM available $N = N_d + N_r$ sub-carriers are shared by data and redundant symbols [1]. N_d sub-carriers are occupied by data symbols and remaining N_r sub-carriers are dedicated to redundant symbols. Therefore the frequency domain symbol vector $\tilde{\mathbf{x}} \in \mathbb{C}^{N\times 1}$ can be denoted as consisting of data and redundant parts $\tilde{\mathbf{x}} = \begin{bmatrix}\tilde{\mathbf{d}}^H & \tilde{\mathbf{x}}_r^H\end{bmatrix}^H$, where $\tilde{\mathbf{d}}^H \in \mathbb{C}^{N_d\times 1}$ is the part reserved for data, and $\tilde{\mathbf{x}}_r^H \in \mathbb{C}^{N_r\times 1}$ contains redundancy. UW is generated in two steps [1]:

1) A zero UW is generated, such that the time domain OFDM symbol vector is given as $\mathbf{x} = \begin{bmatrix}\mathbf{x}_d^H & \mathbf{0}\end{bmatrix}^H$ and $\mathbf{x} = \frac{1}{N}\mathbf{F}_N^H\tilde{\mathbf{x}}$.

2) The nonzero UW $\mathbf{x}_u^H \in C^{N_r \times 1}$ is added in the time domain, resulting in $\mathbf{x}' = \mathbf{x} + \begin{bmatrix}\mathbf{0} & \mathbf{x}_u^H\end{bmatrix}^H$.

The redundancy is added during the first step, and it is considered in detail here. The IFFT operation on the frequency domain symbol vector must yield

$$\frac{1}{N}\mathbf{F}_N^H\mathbf{P}\begin{bmatrix}\tilde{\mathbf{d}}\\ \tilde{\mathbf{x}}_r\end{bmatrix} = \begin{bmatrix}\mathbf{x}_d\\ \mathbf{0}\end{bmatrix} \tag{1}$$

Here, $\mathbf{P}$ is the introduced permutation matrix that allocates data and redundant sub-carriers in such a way that energy contribution of the redundant sub-carrier symbols is minimal. The matrix in Eq. 1 can be renamed as $\frac{1}{N}\mathbf{F}_N^H\mathbf{P} = \mathbf{M} = \begin{bmatrix}\mathbf{M}_{11} & \mathbf{M}_{12}\\ \mathbf{M}_{21} & \mathbf{M}_{22}\end{bmatrix}$, where $\mathbf{M}_{ij}$ are sub-matrices of an appropriate size. From matrix multiplication in Eq. 1

$$\mathbf{M}_{21}\tilde{\mathbf{d}} + \mathbf{M}_{22}\tilde{\mathbf{x}}_r = \mathbf{0}$$

The generation of redundant sub-carrier symbols $\tilde{\mathbf{x}}_r$ from the data symbols follows directly as

$$\tilde{\mathbf{x}}_r = \mathbf{T}\tilde{\mathbf{d}} \tag{2}$$

where $\mathbf{T} = -\mathbf{M}_{22}^{-1}\mathbf{M}_{21}$, $\mathbf{T} \in \mathbb{C}^{N_r \times N_d}$.

In style of block coding theory, the frequency domain symbol vector $\tilde{\mathbf{x}}$ can be interpreted as a code word of a complex RS (Reed-Solomon)-code [3],

$$\tilde{\mathbf{x}} = \mathbf{P}\begin{bmatrix}\tilde{\mathbf{d}}\\ \tilde{\mathbf{x}}_r\end{bmatrix} = \mathbf{P}\begin{bmatrix}\mathbf{I}\\ \mathbf{T}\end{bmatrix}\tilde{\mathbf{d}} = \mathbf{G}\tilde{\mathbf{d}} \tag{3}$$

where $\mathbf{G} \in \mathbb{C}^{(N_d+N_r)\times N_d}$ is the code generator matrix that introduces correlations within the symbol vector $\tilde{\mathbf{x}}$. The interpretation as the RS code is valid, because it is defined as a set of codewords whose Fourier transform produces a consecutive set of zeroes. This is exactly the case in Eq. 1, with the only difference that the encoding is performed on the set of complex numbers [4].

The second step of signal generation adds UW in the time domain, resulting in transmit UW-OFDM symbol vector $\mathbf{x}'$. The frequency domain version $\tilde{\mathbf{x}}_u \in \mathbb{C}^{N_r \times 1}$ of the non-zero unique word is obtained as $\tilde{\mathbf{x}}_u = \mathbf{F}_N\begin{bmatrix}\mathbf{0} & \mathbf{x}_u^H\end{bmatrix}^H$.

This allows the transmit time domain symbol vector to be rewritten as

$$\mathbf{x}' = \frac{1}{N}\mathbf{F}_N^H(\tilde{\mathbf{x}} + \tilde{\mathbf{x}}_u) = \frac{1}{N}\mathbf{F}_N^H(\mathbf{G}\tilde{\mathbf{d}} + \tilde{\mathbf{x}}_u) \tag{4}$$

The received frequency domain symbol vector is then given as

$$\tilde{\mathbf{y}} = \tilde{\mathbf{H}}_d\mathbf{G}\tilde{\mathbf{d}} + \tilde{\mathbf{H}}_d\tilde{\mathbf{x}}_u + \tilde{\mathbf{n}} \tag{5}$$

Next, after subtracting the known part $\tilde{\mathbf{H}}_d\tilde{\mathbf{x}}_u$, the system equation for UW-OFDM is given as

$$\tilde{\mathbf{y}}' = \tilde{\mathbf{H}}_d\mathbf{G}\tilde{\mathbf{d}} + \tilde{\mathbf{n}} \tag{6}$$

The matrix $\tilde{\mathbf{H}}_d$ is diagonal, containing the flat fading channel coefficients on the main diagonal. This matrix is defined by the cyclicity of the UW-OFDM frame due to repeating UWs. In that sense, the only difference between UW- and CP-OFDM in terms of receiver is the presence of the generator matrix $\mathbf{G}$.

B. Non-systematic generation of UW

As opposed to systematic UW generation, where the redundancy is placed at dedicated sub-carriers, non-systematic UW generation spreads the redundancy among all sub-carriers [4]. The generator matrix is now denoted $\bar{\mathbf{G}}$, and is given as

$$\bar{\mathbf{G}} = \mathbf{A}\mathbf{P}\begin{bmatrix}\mathbf{I}\\ \bar{\mathbf{T}}\end{bmatrix} \tag{7}$$

where $\mathbf{A} \in \mathbb{R}^{(N_d+N_r)\times(N_d+N_r)}$ is a non-singular real matrix, and permutation matrix $\mathbf{P}$ is same as with the systematic UW generation. The generator matrix still has to produce zeroes at the positions of N_r symbols in the time domain analogous to Eq. 1.

$$\frac{1}{N}\mathbf{F}_N^H\mathbf{A}\mathbf{P}\begin{bmatrix}\mathbf{I}\\ \bar{\mathbf{T}}\end{bmatrix}\tilde{\mathbf{d}} = \begin{bmatrix}\mathbf{x}_d\\ \mathbf{0}\end{bmatrix} \tag{8}$$

Introducing $\bar{\mathbf{M}} = \frac{1}{N}\mathbf{F}_N^H\mathbf{A}\mathbf{P} = \begin{bmatrix}\bar{\mathbf{M}}_{11} & \bar{\mathbf{M}}_{12}\\ \bar{\mathbf{M}}_{21} & \bar{\mathbf{M}}_{22}\end{bmatrix}$, Eq. 8 can be fulfilled by choosing $\bar{\mathbf{T}} = -\bar{\mathbf{M}}_{22}^{-1}\bar{\mathbf{M}}_{21}$. The optimum value of matrix $\mathbf{A}$, such that Eq. 8 is fulfilled, is obtained in [4] by the steepest descent algorithm. Two initializations are proposed:

1) Initialization with identity matrix

$$\mathbf{A}^{(0)} = \mathbf{I} \tag{9}$$

implying $\bar{\mathbf{T}}^{(0)} = \mathbf{T}$ and

$$\bar{\mathbf{G}}^{(0)} = \mathbf{P}\begin{bmatrix}\mathbf{I} & \mathbf{T}^H\end{bmatrix}^H = \mathbf{G} \tag{10}$$

Therefore, iterative search starts with the systematic generator matrix, which is considered a reasonable choice. After optimization, the resulting generator matrix is obtained and denoted $\mathbf{G}'$.

2) Random initialization. Each element of $\mathbf{A}^{(0)}$ is a Gaussian random variable with zero mean and variance one.

$$a_{ij}^{(0)} \sim N(0,1) \tag{11}$$

The resulting generator matrix is in this case denoted as $\mathbf{G}''$.

As the obtained generator matrix distributes portions of a single data symbol over a number of codeword symbols it can be interpreted as a combination of channel independent precoder and a channel encoder [4].

Different generator matrices introduce another degree of freedom to the system Eq. 6. By considering the compound matrix $\tilde{\mathbf{H}}_d\mathbf{G}$ as a synthetic channel matrix, SISO UW-OFDM can be regarded as a MIMO system. SISO UW-OFDM therefore benefits from both inherent encoding and MIMO detection

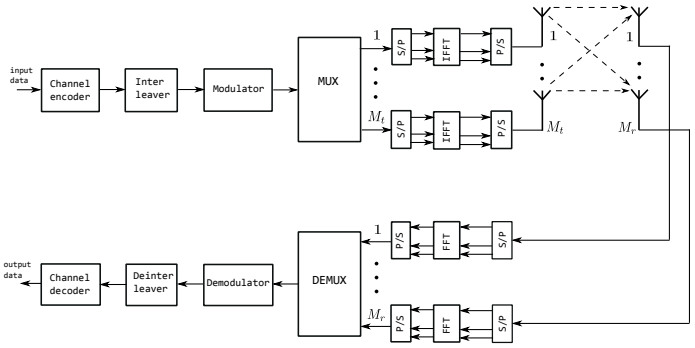

Fig. 2: MIMO OFDM transceiver

algorithms. Obviously, these algorithms are not applicable to SISO CP-OFDM. Therefore, it makes sense to generalize UW-OFDM to a MIMO system and compare its performance against MIMO CP-OFDM.

III. MIMO UW-OFDM

Consider a MIMO OFDM transceiver block diagram depicted in Fig. 2. There are M_t parallel data symbol vectors $\tilde{\mathbf{d}}_m$, $m = 1, \ldots, M_t$, transmitted simultaneously over M_t transmit antennas. Hence, on each k-th sub-carrier, $k = 1, \ldots, N_d$, the M_t data symbols from the respective data symbol vectors are transmitted simultaneously over M_t antennas. Therefore, the data occupying sub-carrier k is a vector, given as

$$\tilde{\mathbf{d}}(k) = \begin{bmatrix} \tilde{d}_1(k) \\ \vdots \\ \tilde{d}_{M_t}(k) \end{bmatrix}_{M_t \times 1} \tag{12}$$

The overall vector of transmitted symbols with respect to sub-carriers and transmit antennas is denoted as

$$\tilde{\mathbf{d}} = \begin{bmatrix} \tilde{\mathbf{d}}(1) \\ \vdots \\ \tilde{\mathbf{d}}(N_d) \end{bmatrix}_{M_t N_d \times 1} \tag{13}$$

where $\tilde{\mathbf{d}}(k)$ is as in Eq. 12. The generation of encoded frequency domain symbol vector $\tilde{\mathbf{x}} \in \mathbb{C}^{N M_t \times 1}$ is done as in Eq. 3. The difference is that the generator matrix $\mathbf{G}$ has to be augmented to correct size by the Kronecker product with identity matrix $\mathbf{I}_{M_t}$,

$$\tilde{\mathbf{x}} = (\mathbf{G} \otimes \mathbf{I}_{M_t})\tilde{\mathbf{d}} = \check{\mathbf{G}}\tilde{\mathbf{d}} \tag{14}$$

where $\check{\mathbf{G}} \in \mathbb{C}^{N M_r \times N_d M_t}$ is the augmented generator matrix.

Random initialization introduced in Sec. II-B produces different non-systematic generator matrices $\mathbf{G}''$. It allows encoding individual streams with different generator matrices $\mathbf{G}''_m$, $m = 1, \ldots, M_t$. In this case the frequency domain symbol vector is obtained as

$$\tilde{\mathbf{x}} = \check{\mathbf{G}}''_s \tilde{\mathbf{d}} \tag{15}$$

where $\check{\mathbf{G}}''_s$ is generated as follows

$$\check{\mathbf{G}}''_s = \left(\mathbf{G}''_1 \otimes \begin{bmatrix} 1 & 0 & \cdots & 0 \\ 0 & 0 & \cdots & 0 \\ \vdots & \vdots & \ddots & \vdots \\ 0 & 0 & \cdots & 0 \end{bmatrix} + \ldots \right. \tag{16}$$

$$\left. \ldots + \mathbf{G}''_{M_t} \otimes \begin{bmatrix} 0 & 0 & \cdots & 0 \\ 0 & 0 & \cdots & 0 \\ \vdots & \vdots & \ddots & \vdots \\ 0 & 0 & \cdots & 1 \end{bmatrix} \right)$$

The transformation to the time domain is performed by M_t parallel IFFT blocks. Mathematically, this parallel operation is expressed as the Kronecker product of the IFFT matrix and identity matrix of size M_t - $\frac{1}{N}(\mathbf{F}_N^H \otimes \mathbf{I}_{M_t})$. The overall time domain symbol vector is obtained similar to the SISO case

$$\mathbf{x} = \frac{1}{N}(\mathbf{F}_N^H \otimes \mathbf{I}_{M_t})\check{\mathbf{G}}\tilde{\mathbf{d}} \tag{17}$$

Next, the vector of non-zero UWs is added to $\mathbf{x}$, as in the SISO UW case.

$$\mathbf{x}' = \mathbf{x} + \begin{bmatrix} \mathbf{0} & \mathbf{x}_u^H \end{bmatrix}^H \tag{18}$$

Where the vector of nonzero-UWs is given as

$$\mathbf{x}_u = \begin{bmatrix} \mathbf{x}_u(N_d + 1) \\ \vdots \\ \mathbf{x}_u(N) \end{bmatrix}_{M_t N_r \times 1}$$

The frequency domain version of the unique word vector is then given as

$$\tilde{\mathbf{x}}_u = (\mathbf{F}_N \otimes \mathbf{I}_{M_t}) \begin{bmatrix} \mathbf{0} & \mathbf{x}_u^H \end{bmatrix}^H \tag{19}$$

leading to the following overall transmit symbol vector

$$\mathbf{x}' = \frac{1}{N}(\mathbf{F}_N^H \otimes \mathbf{I}_{M_t})(\check{\mathbf{G}}\tilde{\mathbf{d}} + \tilde{\mathbf{x}}_u) \tag{20}$$

At the receiver side, the frequency domain receive symbol vector is given as

$$\tilde{\mathbf{y}} = \tilde{\mathbf{H}}_b \check{\mathbf{G}}\tilde{\mathbf{d}} + \tilde{\mathbf{H}}_b \tilde{\mathbf{x}}_u + \tilde{\mathbf{n}} \tag{21}$$

where $\tilde{\mathbf{H}}_b$ is the block diagonal matrix. This matrix is obtained with the same characteristics as in the case of MIMO CP-OFDM, due to cyclicity of UW frames. It contains blocks $\tilde{\mathbf{H}}_b(k) \in \mathbb{C}^{M_r \times M_t}$, filled with flat fading channel coefficients relative to sub-carrier k, $k = 1, \ldots, N$.

Subtracting the known part $\tilde{\mathbf{H}}_b \tilde{\mathbf{x}}_u$ from the receive symbol vector, yields the MIMO UW-OFDM system equation

$$\tilde{\mathbf{y}}' = \tilde{\mathbf{H}}_b \check{\mathbf{G}}\tilde{\mathbf{d}} + \tilde{\mathbf{n}} \tag{22}$$

IV. Detection

A. Linear detection

Linear detection seeks to find an estimate of the transmit symbol vector by linearly combining the elements of the receive symbol vector. It is employed in MIMO systems due to its simplicity and sufficient BER performance. Among linear schemes, linear minimum mean square error (LMMSE) detection performs the best [9].

The LMMSE estimate for MIMO UW-OFDM system equation is given as

$$\hat{\tilde{\mathbf{d}}}_{\text{lmmse}} = \left(\check{\mathbf{G}}^H \tilde{\mathbf{H}}_b^H \tilde{\mathbf{H}}_b \check{\mathbf{G}} + \frac{N\sigma_n^2}{\sigma_d^2}\mathbf{I}\right)^{-1} \check{\mathbf{G}}^H \tilde{\mathbf{H}}_b^H \tilde{\mathbf{y}}' \tag{23}$$

where σ_n^2 is the noise variance, and σ_d^2 is the data variance [10].

Due to correlation between sub-carriers introduced by generator matrix $\check{\mathbf{G}}$, the LMMSE estimate is calculated once for all sub-carriers and data streams. In case of MIMO CP-OFDM, the system equation 22 lacks the generator matrix and is of the form

$$\tilde{\mathbf{y}} = \tilde{\mathbf{H}}_b \tilde{\mathbf{x}} + \tilde{\mathbf{n}} \tag{24}$$

In this case, the LMMSE estimate is computed for N sub-equations $\tilde{\mathbf{y}}(k) = \tilde{\mathbf{H}}_b(k)\tilde{\mathbf{x}}(k) + \tilde{\mathbf{n}}(k)$ due to the block diagonal structure of $\tilde{\mathbf{H}}_b$. However, it is to note that in the case of MIMO UW-OFDM the size of the matrix to be inverted has increased from $M_r \times M_t$ to less favorable $N_d M_r \times N_d M_t$.

1) Soft output generation for LMMSE: In order to obtain good performance in the coded system, reliability information should be passed from the detector to the channel decoder. The reliability information for each bit $b_{i,j}$ is expressed as log likelihood ratio (LLR)

$$\begin{aligned} L(b_{i,j}) &= \ln \frac{Pr(b_{i,j}=1|\tilde{\mathbf{y}}', \tilde{\mathbf{H}}_b\check{\mathbf{G}})}{Pr(b_{i,j}=0|\tilde{\mathbf{y}}', \tilde{\mathbf{H}}_b\check{\mathbf{G}})} \\ &= \ln \left(\frac{\sum\limits_{\tilde{\mathbf{d}}\in\chi_{i,j}^1} p(\tilde{\mathbf{y}}'|\tilde{\mathbf{d}}, \tilde{\mathbf{H}}_b\check{\mathbf{G}})}{\sum\limits_{\tilde{\mathbf{d}}\in\chi_{i,j}^0} p(\tilde{\mathbf{y}}'|\tilde{\mathbf{d}}, \tilde{\mathbf{H}}_b\check{\mathbf{G}})} \right) \end{aligned} \tag{25}$$

where $\chi_{i,j}^1$ and $\chi_{i,j}^0$ are sets of all transmit symbol vectors with bit position j at symbol i equal to 1 or 0 respectively. The number of terms that have to be evaluated in Eq. 25 equals $2^{n_b N_d M_t}$, where n_b is the number of bits per modulation symbol.

Using the max-log approximation ($\ln \sum_s a_s = \max a_s$) [11], Eq. 25 is simplified as given below

$$L(b_{i,j}) \approx \frac{\left(\min\limits_{\tilde{\mathbf{d}}\in\chi_{i,j}^0} \|\tilde{\mathbf{y}}' - \tilde{\mathbf{H}}_b\check{\mathbf{G}}\tilde{\mathbf{d}}\|_2^2 - \min\limits_{\tilde{\mathbf{d}}\in\chi_{i,j}^1} \|\tilde{\mathbf{y}}' - \tilde{\mathbf{H}}_b\check{\mathbf{G}}\tilde{\mathbf{d}}\|_2^2 \right)}{N\sigma_n^2} \tag{26}$$

Now, a direct computation of probabilities and logarithm is eliminated, but still $2^{n_b N_d M_t}$ Euclidean distances need to be computed.

Further simplification was proposed in [12]. Instead of computing LLR on the receive vector, the output $\hat{\mathbf{d}}$ of the LMMSE is considered. The resulting LLR is now of the form

$$L_l(b_{i,j}) \approx \frac{1}{\sigma_e^2} \left(\min_{\tilde{d}_i\in\chi_j^0} |\hat{\tilde{d}}_i - \tilde{d}_i|^2 - \min_{\tilde{d}\in\chi_j^1} |\hat{\tilde{d}}_i - \tilde{d}_i|^2 \right) \tag{27}$$

where σ_e^2 is the diagonal element of the MMSE matrix $\mathbf{C}_{ee}$, given as

$$\mathbf{C}_{ee} = N\sigma_n^2 \left(\check{\mathbf{G}}^H \tilde{\mathbf{H}}_b^H \tilde{\mathbf{H}}_b \check{\mathbf{G}} + \frac{N\sigma_n^2}{\sigma_d^2}\mathbf{I} \right)^{-1} \tag{28}$$

For example, in the case of 4-QAM and Gray mapping, the LLRs are computed separately for in-phase and quadrature components

$$\begin{aligned} \Re\{L_l(\tilde{d}_i)\} &= \frac{4}{\sigma_e^2}\Re\{\hat{\tilde{d}}_i\} \\ \Im\{L_l(\tilde{d}_i)\} &= \frac{4}{\sigma_e^2}\Im\{\hat{\tilde{d}}_i\} \end{aligned} \tag{29}$$

B. Maximum Likelihood detection

Maximum likelihood detection is performed by minimizing the Euclidean distance between the receive signal vector $\tilde{\mathbf{y}}'$ and transmit symbol vector $\tilde{\mathbf{d}}$, as expressed in Eq. 30

$$\hat{\tilde{\mathbf{d}}}_{\text{ML}} = \underset{\tilde{\mathbf{d}}\in\mathbb{A}^{N_d M_t}}{\operatorname{argmin}} \|\tilde{\mathbf{y}}' - \tilde{\mathbf{H}}_b\check{\mathbf{G}}\tilde{\mathbf{d}}\|_2^2 \tag{30}$$

where $\mathbb{A}$ is the modulation alphabet.

1) Sphere Decoding: Sphere decoding maps Eq. 30 to a tree search. However, in the case of MIMO UW-OFDM, the size of transmit symbol vector is $N_d M_t \times 1$, leading to a very large tree and prohibitive complexity. It has already been mentioned that SD has been applied to SISO UW-OFDM [5], [13]. However, the number of sub-carriers had to be restricted to $N = 24$.

Therefore, SD will only be used for MIMO CP-OFDM detection in this work. It will provide a ML performance reference for MIMO-UW OFDM. The SD implementation used in this paper is the one given in [14], with initial sphere radius set to infinity. Soft output generation is performed as in [15].

2) Likelihood Ascent Search: Likelihood Ascent Search (LAS) is the quasi-Maximum likelihood detection algorithm developed for massive MIMO systems [7], [8], [16]. Therefore, it is a natural candidate for MIMO UW-OFDM.

The algorithm performs a sequence of local searches based on an initial solution vector in order to arrive as close as possible to the ML solution. In local search, a neighborhood of the initial solution is defined as a set of vectors that differ from initial vector in η positions. In general, the size of η-

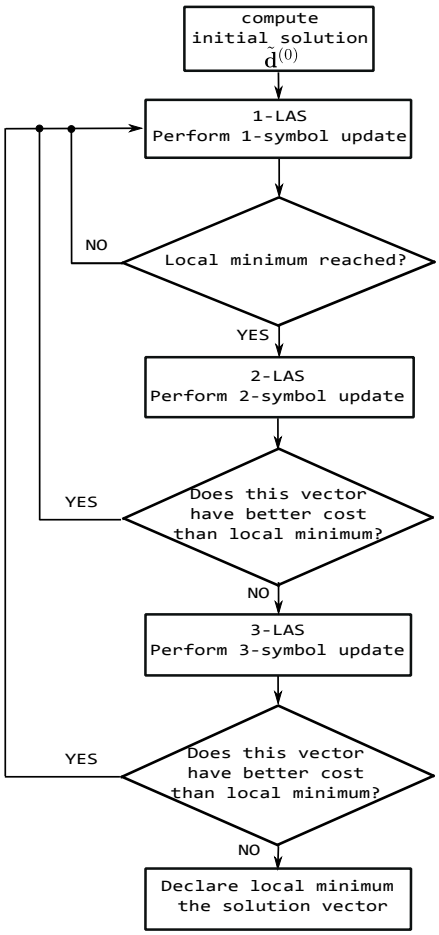

Fig. 3: Stateflow of 3-LAS algorithm

neighborhood is given as

$$|S_\eta(\tilde{\mathbf{d}})| = \binom{N_d M_t}{\eta} \tag{31}$$

In case $\eta = N_d M_t$, the neighborhood contains all possible solution vectors, and the search within this neighborhood corresponds to the global search. It has been shown that the local search provides good results for $\eta \leq 3$ for massive MIMO systems with hundreds of antennas [7].

The basic version, denoted 1-LAS, searches for the vector from $S_1(\tilde{\mathbf{d}})$ with minimum ML metric and declares it the final ML solution. This solution, however, represents the ML solution in 1-neighborhood, and most likely is a local minimum.

The local minimum escape strategy is to perform limited $S_2(\tilde{\mathbf{d}})$, and if necessary, $S_3(\tilde{\mathbf{d}})$ neighborhood searches. If these searches increase the likelihood, the escape was successful and 1-neighborhood search starts over. This version is denoted as η-LAS, and its flowchart is depicted in Fig. 3, for $\eta = 3$.

Next, 1-LAS search procedure is elaborated in detail [17]. The system equation (Eq. 22) is transformed to real-valued domain as follows:

$$\begin{bmatrix} \Re(\tilde{\mathbf{y}}') \\ \Im(\tilde{\mathbf{y}}') \end{bmatrix} = \begin{bmatrix} \Re(\tilde{\mathbf{H}}_b\check{\mathbf{G}}) & -\Im(\tilde{\mathbf{H}}_b\check{\mathbf{G}}) \\ \Im(\tilde{\mathbf{H}}_b\check{\mathbf{G}}) & \Re(\tilde{\mathbf{H}}_b\check{\mathbf{G}}) \end{bmatrix} \begin{bmatrix} \Re(\tilde{\mathbf{d}}) \\ \Im(\tilde{\mathbf{d}}) \end{bmatrix} + \begin{bmatrix} \Re(\tilde{\mathbf{n}}) \\ \Im(\tilde{\mathbf{n}}) \end{bmatrix} \tag{32}$$

The initial solution to 1-LAS is the LMMSE estimate, quantized to the nearest neighbor $\tilde{\mathbf{d}} \in \mathbb{A}^{2N_d M_t}$.

$$\tilde{\mathbf{d}}^{(0)} = \mathcal{Q}(\hat{\tilde{\mathbf{d}}}_{\text{lmmse}}) \tag{33}$$

The ML cost function after m-th iteration is given by

$$C^{(m)} = \|\tilde{\mathbf{y}}' - \tilde{\mathbf{H}}_b\check{\mathbf{G}}\tilde{\mathbf{d}}^{(m)}\|_2^2 \tag{34}$$

$$= \tilde{\mathbf{d}}^{(m)^T}\check{\mathbf{G}}^T\tilde{\mathbf{H}}_b^T\tilde{\mathbf{H}}_b\check{\mathbf{G}}\tilde{\mathbf{d}}^{(m)} - 2\tilde{\mathbf{y}}'^T\tilde{\mathbf{H}}_b\check{\mathbf{G}}\tilde{\mathbf{d}}^{(m)} \tag{35}$$

Assume the symbol position $p = 1, \ldots, 2N_d M_t$ is updated in $(m+1)$-th iteration. The update rule is given as

$$\tilde{\mathbf{d}}^{(m+1)} = \tilde{\mathbf{d}}^{(m)} + \lambda_p^{(m)}\mathbf{e}_p \tag{36}$$

where $\mathbf{e}_p$ is the unit vector with p-th entry set to one. The value of $\lambda^{(m)}$ depends on the modulation used and can be obtained analytically for any modulation scheme [17]. In case of 4-QAM, it takes only two possible values

$$\lambda_p^{(m)} = \begin{cases} -2 & \text{when } d_p^{(m)} = +1 \\ +2 & \text{when } d_p^{(m)} = -1 \end{cases} \tag{37}$$

Defining matrix $\mathbf{W} = \check{\mathbf{G}}\tilde{\mathbf{H}}_b^T\tilde{\mathbf{H}}_b\check{\mathbf{G}}$, the cost difference can be written as

$$\Delta C_p^{m+1} = C^{(m+1)} - C^{(m)} = {\lambda_p^{(m)}}^2 w_{pp} - 2\lambda_p^{(m)} z_p^{(m)} \tag{38}$$

where $z_p^{(m)}$ is the p-th entry of $\mathbf{z}^{(m)} = \check{\mathbf{G}}\tilde{\mathbf{H}}_b^T(\tilde{\mathbf{y}}' - \tilde{\mathbf{H}}_b\check{\mathbf{G}}\tilde{\mathbf{d}}^{(m)})$, and w_{pp} is the (p,p)- th entry of matrix $\mathbf{W}$.

Next, index s of position with minimum ML cost difference $s = \underset{p=1,\ldots,2N_d M_t}{\operatorname{argmin}} \Delta C_p^{m+1}$ is obtained. If $\Delta C_s^{m+1} < 0$, the solution vector and vector $\mathbf{z}$ are updated as follows.

$$\tilde{\mathbf{d}}^{(m+1)} = \tilde{\mathbf{d}}^{(m)} + \lambda_s^{(m)} z_s^{(m)}\mathbf{e}_s \tag{39}$$

$$\mathbf{z}^{(m+1)} = \mathbf{z}^{(m)} - \lambda_s^{(m)} z_s^{(m)}\mathbf{w}_s \tag{40}$$

where $\mathbf{w}_s$ is the s-th column of matrix $\mathbf{W}$. If $\Delta C_s^{m+1} > 0$, then 1-symbol update local minimum is reached, and the search is terminated. The resulting vector $\tilde{\mathbf{d}}$ is the solution of 1-LAS algorithm. An escape from local minimum is attempted by performing two or three symbol updates. The respective update procedures are similar and are described in detail in [7], [17].

a) Soft output generation: Soft output generation is proposed in [17]. The reliability information for each bit is formulated as

$$R(b_{i,j}) \approx \frac{\|\tilde{\mathbf{y}}' - \tilde{\mathbf{H}}_b\check{\mathbf{G}}\hat{\tilde{\mathbf{d}}}_i^{j-}\|_2^2 - \|\tilde{\mathbf{y}}' - \tilde{\mathbf{H}}_b\check{\mathbf{G}}\hat{\tilde{\mathbf{d}}}_i^{j+}\|_2^2}{\|(\tilde{\mathbf{h}}_b\check{\mathbf{g}})_i\|_2^2} \tag{41}$$

where $\hat{\tilde{\mathbf{d}}}_i^{j-}$ and $\hat{\tilde{\mathbf{d}}}_i^{j+}$ are the LAS solution vectors with j-th bit of symbol i set to -1 or $+1$ respectively, $(\tilde{\mathbf{h}}_b\check{\mathbf{g}})_i$ is the i-th column of $\tilde{\mathbf{H}}_b\check{\mathbf{G}}$. It is to note that the soft output in Eq. 41 represents a very coarse approximation of max-log LLR in

Eq. 26, as other vectors belonging to $\chi_{i,j}^{1}$ and $\chi_{i,j}^{0}$ are simply neglected.

The soft output in Eq. 41 is then efficiently reformulated in terms of $\mathbf{z}$ and $\mathbf{W}$, which are readily available after the termination of LAS algorithm. Note that $\hat{\tilde{\mathbf{d}}}_i^{j-}$ and $\hat{\tilde{\mathbf{d}}}_i^{j+}$ differ only in the i-th entry, and hence

$$\hat{\tilde{\mathbf{d}}}_i^{j-} = \hat{\tilde{\mathbf{d}}}_i^{j+} + \lambda_{i,j}\mathbf{e}_i \tag{42}$$

Substituting Eq. 42 in Eq. 41 yields

$$R(b_{i,j}) = \begin{cases} \lambda_{i,j}^2 - 2\lambda_{i,j}\frac{z_i}{w_{ii}} & \text{when } b_{i,j} = +1 \\ -\lambda_{i,j}^2 - 2\lambda_{i,j}\frac{z_i}{w_{ii}} & \text{when } b_{i,j} = -1 \end{cases} \tag{43}$$

It turns out that the quality of proposed soft outputs is not adequate for coded MIMO UW-OFDM. The performance of LAS in this case is worse than that of the LMMSE initial solution. The problem with this version of LAS algorithm is that it quantizes the LMMSE output, thus ignoring the LLR provided by LMMSE (Eq. 27). Therefore, for use in the coded system the LAS algorithm has to be modified.

b) Proposed modified LAS for coded system: As LAS is essentially an improvement of the LMMSE solution, the LLR provided by LMMSE can be used as a-priori information. Assuming 4-QAM with Gray mapping and as LAS operates on real-valued system equation 32, $d_i = b_i$. Hence, the initial ML cost is given as

$$C^{(0)} = \|\tilde{\mathbf{y}}' - \tilde{\mathbf{H}}_b\check{\mathbf{G}}\tilde{\mathbf{d}}^{(0)}\|_2^2 - \ln(Pr(\tilde{\mathbf{d}}^{(0)})) \tag{44}$$

where $Pr(\tilde{\mathbf{d}}) = \prod_{i=1}^{2N_dM_t} Pr(\tilde{d}_i)$ is the a-priori probability of transmit data vector $\tilde{\mathbf{d}}$. Changing symbol at position p results in the probability change for that symbol from $Pr(\tilde{d}_p)$ to $Pr(\bar{\tilde{d}}_p)$. Here, symbol $\bar{\tilde{d}}_p$ represents the sign flipped version of symbol $\tilde{d}_p$. Therefore, the change in ML cost from iteration m to $m+1$ is given as

$$\begin{aligned} &\Delta C_p^{m+1} = C^{(m+1)} - C^{(m)} = \\ &= {\lambda_p^{(m)}}^2 w_{pp} - 2\lambda_p^{(m)} z_p^{(m)} + \ln(Pr(\tilde{d}_p)) - \ln(Pr(\bar{\tilde{d}}_p)) \end{aligned} \tag{45}$$

The probabilities of symbols at positions different from p remain the same, and are canceled out in the subtraction. Symbol probabilities $Pr(\tilde{d}_p)$ and $Pr(\bar{\tilde{d}}_p)$ are easily obtained from $L_l(\tilde{d}_i)$ as [18]

$$Pr(\tilde{d}_p = +1) = \frac{\exp(L_l(\tilde{d}_p))}{1+\exp(L_l(\tilde{d}_p))} \tag{46}$$

$$Pr(\tilde{d}_p = -1) = \frac{1}{1+\exp(L_l(\tilde{d}_p))} \tag{47}$$

After the modified LAS terminates, the soft outputs are generated as

$$L_{\text{new}}(\tilde{d}_i) = \begin{cases} \hat{\tilde{d}}_i & \text{when } sign(\hat{\tilde{d}}_i) \neq sign(L_l(\tilde{d}_i)) \\ L_l(\tilde{d}_i) & \text{when } sign(\hat{\tilde{d}}_i) = sign(L_l(\tilde{d}_i)) \end{cases} \tag{48}$$

In case LAS changes the symbol, its hard-decision value is taken as the soft output. In case the symbol is not changed, the LLR provided by LMMSE initial solution is used.

c) LAS performance improvement in case of $\check{\mathbf{G}}_s''$: Systematic and non-systematic generator matrices alter the block channel matrix $\tilde{\mathbf{H}}_b$ in a different way. Figure 4 depicts the virtual channel matrices for three possible cases.

In case of systematic generator matrix, virtual channel matrix is of a block diagonal form. In case of the non-systematic generator matrix, obtained from the systematic one, virtual channel matrix $\tilde{\mathbf{H}}_b\check{\mathbf{G}}'$ still possesses the block diagonal-like form. In case of the generator matrix obtained from random initialization, the virtual channel matrix $\tilde{\mathbf{H}}_b\check{\mathbf{G}}''$ is a full matrix. This explains why the performance of the uncoded system using matrix $\check{\mathbf{G}}''$ is superior to the one using matrices $\check{\mathbf{G}}'$ or $\check{\mathbf{G}}$.

As far as LAS is concerned, its performance degrades when the channel matrix is correlated [17]. This is essentially the case for UW-OFDM, as the generator matrix introduces correlations between diagonal blocks of $\tilde{\mathbf{H}}_b$. Therefore, by using generator matrix $\check{\mathbf{G}}_s''$, introduced correlation is less, as this matrix is made of M_t distinct $\check{\mathbf{G}}''$. It is then to expect that using $\check{\mathbf{G}}_s''$ would bring additional LAS performance improvement.

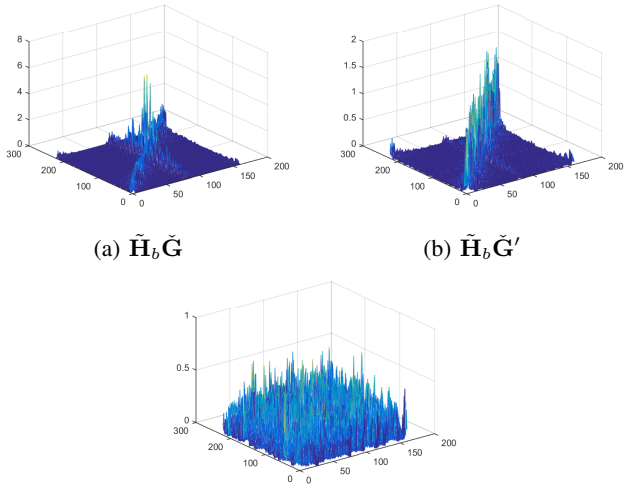

(a) $\tilde{\mathbf{H}}_b\check{\mathbf{G}}$ (b) $\tilde{\mathbf{H}}_b\check{\mathbf{G}}'$

(c) $\tilde{\mathbf{H}}_b\check{\mathbf{G}}''$

Fig. 4: Virtual channel matrices

V. Results

A. Simulation parameters

Parameters of the UW-OFDM system are where possible picked the same as in CP-OFDM based 802.11n standard. The system parameters are summarized in Table I.

TABLE I: MIMO system parameters

OFDM system		802.11n	UW
FFT size	N	64	64
data subcarriers	N_d	52	40
guard interval/ redundant subcarriers	N_g/ N_r	16	16
red. subcarrier indices	$\mathcal{I}_r$	{}	{2, 6, 10, 14, 17, 21, 24, 26, 38, 40, 43, 47, 50, 54, 58, 62}
zero subcarriers	N_z	8	8
zero subcarrier indices	$\mathcal{I}_z$	{0, 29, 30,. . . , 35}	
transmit antennas	M_t	4	4
receive antennas	M_r	4	4

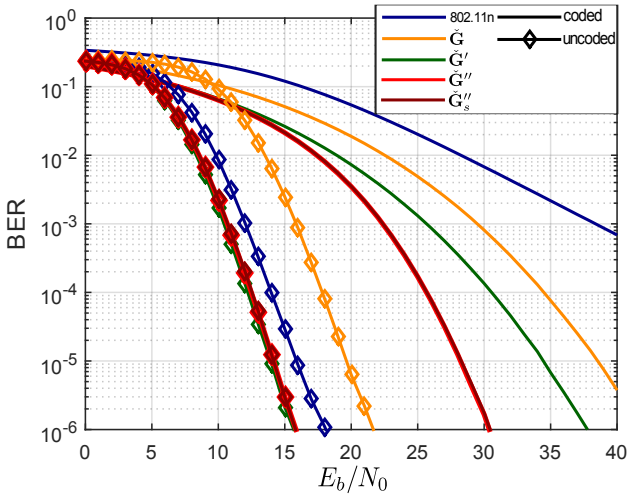

Fig. 5: LMMSE performance.

The recorded 10000 multipath channel realizations are used in all simulations. The channel coefficients are obtained from the standardized 802.11n channel model (model C) [19]. The channel is assumed constant for 100 OFDM symbol vectors. Modulation is 4-QAM with Gray mapping. In case of a coded system, information bits are encoded by (133, 171) convolutional code with constraint length 7 and code rate $1/2$. At the receiver side, the detected bits are decoded by soft decision Viterbi decoder.

B. Simulation results

The bit error rate (BER) results for LMMSE detection are depicted in Figure 5. MIMO UW-OFDM clearly outperforms 802.11n in both uncoded and coded systems. In an uncoded system, using generator matrix $\check{\mathbf{G}}''$ provides maximum gain over 802.11n. In a coded system, UW system with generator matrix $\check{\mathbf{G}}'$ outperforms 802.11n the most. The performance of these generator matrices in coded and uncoded systems coincides with the SISO OFDM case [4].

Figure 6 depicts the gain due to 1-LAS compared to the LMMSE initial solution. It can be observed that UW system with $\check{\mathbf{G}}''$ approaches sphere decoded 802.11n closer than the one with $\check{\mathbf{G}}'$, due to the better performing initial solution. Individual encoding of data streams with $\check{\mathbf{G}}''_s$ further improves 1-LAS performance. It should be noted, that the performance of LMMSE initial solutions for $\check{\mathbf{G}}''$ and $\check{\mathbf{G}}''_s$ is exactly the same.

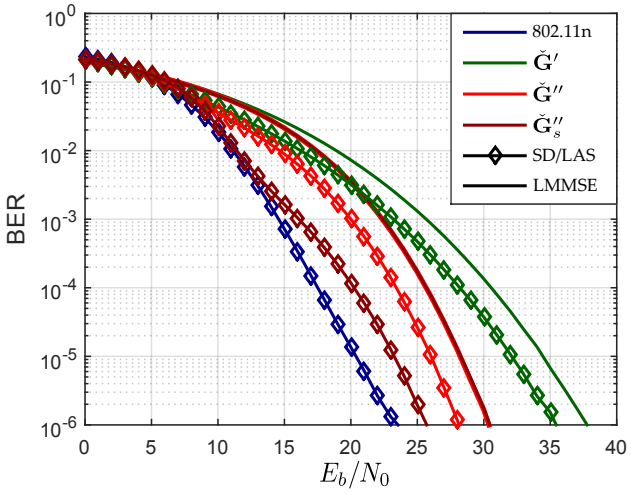

Fig. 6: 1-LAS vs LMMSE, uncoded.

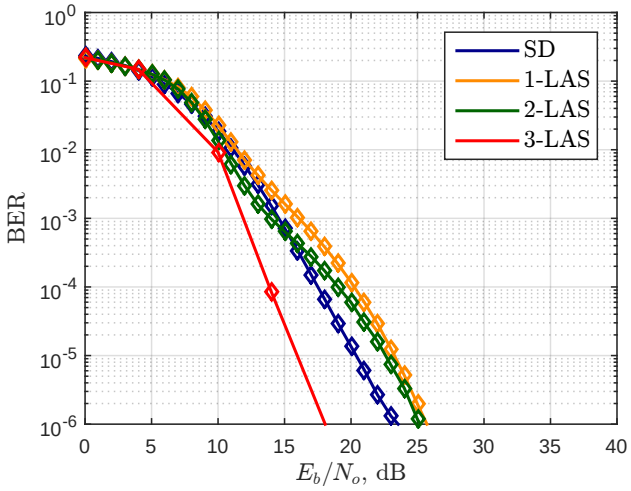

Fig. 7: M-LAS vs SD, $\check{\mathbf{G}}''_s$, uncoded.

Figure 7 depicts performance of three versions of LAS algorithm against sphere decoded 802.11n in an uncoded system. It can be observed that the performance of LAS improves with the number of stages, and with 3-LAS, 802.11n is outperformed by 6 dB at BER of 10^{-6}. Unfortunately, the complexity penalty associated with 3-LAS is not negligible. 3-LAS simulation takes two orders of magnitude more time than the SD 802.11n simulation on the same host. The reason is the size of $S_3(\tilde{\mathbf{d}})$ neighborhood (Eq. 31) that is getting very large, considering parameters given in Table I.

Figure 8 illustrates the problem with initially proposed soft output computation (Eq. 43) for the coded system. In this case, the performance of 1-LAS degrades with respect to the LMMSE solution. As previously mentioned, ignoring reliability information provided by LMMSE, causes this behavior. The proposed modified 1-LAS (Eq. 48) improves the performance of the initial LMMSE solution.

Finally, figure 9 depicts performance of LAS using generator matrix $\check{\mathbf{G}}'$ with respect to SD 802.11n performance. It can

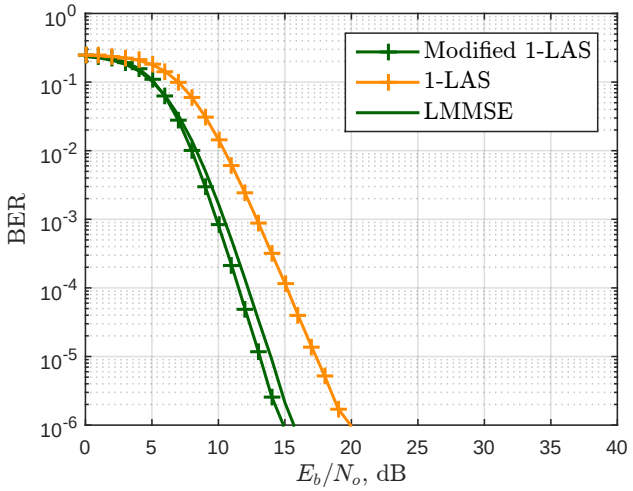

Fig. 8: Proposed modified 1-LAS vs 1-LAS, $\check{\mathbf{G}}'$, coded.

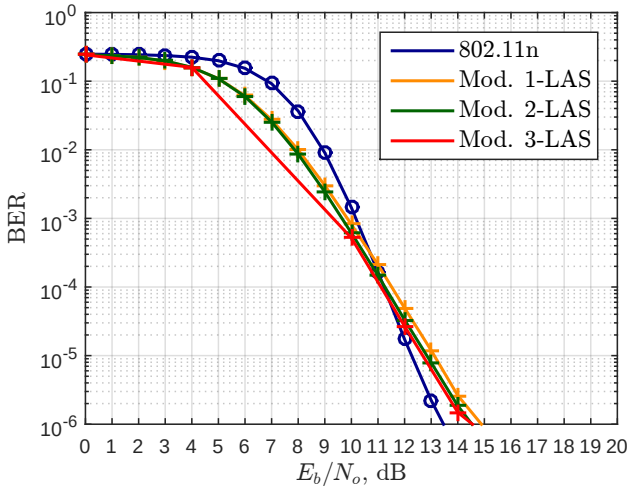

Fig. 9: M-LAS vs SD, $\check{\mathbf{G}}'$, coded.

be observed that, again, performance of LAS improves with the number of stages. However, performance of SD 802.11n cannot be achieved, and there is still a loss of 0.8 dB at BER of 10^{-6} for 3-LAS.

VI. Conclusion

This work addressed the generalization of UW-OFDM to the MIMO case. It has been shown that simple quasi-ML algorithms initially introduced for massive MIMO systems are applicable to MIMO UW with minor modifications. Simulation results indicate that MIMO UW-OFDM outperforms MIMO CP-OFDM in case of linear detection in both coded and uncoded systems.

In case of quasi-ML detection, MIMO UW-OFDM is able to outperform SD MIMO CP-OFDM in the uncoded system. In a coded system, ML MIMO CP-OFDM performance cannot be achieved.

It can be concluded that MIMO UW-OFDM can be used as an intermediate solution between LMMSE MIMO-CP OFDM and ML MIMO CP-OFDM. In case of 1-LAS, MIMO UW-OFDM exhibits lower complexity than ML MIMO CP-OFDM, and is able to achieve close to ML MIMO CP-OFDM performance in both coded and uncoded setups.

References

[1] M. Huemer, C. Hofbauer, and J. B. Huber, "The Potential of Unique Words in OFDM," in *Proceedings of the 15th International OFDM-Workshop 2010 (InOWo' 10)*, Sep. 2010, pp. 140 – 144. [Online]. Available: http://ofdm.tu-harburg.de/index.html

[2] C. Hofbauer and M. Huemer, "A study of data rate equivalent UW-OFDM and CP-OFDM concepts," in *Signals, Systems and Computers (ASILOMAR), 2012 Conference Record of the Forty Sixth Asilomar Conference on*, Nov 2012, pp. 173–177.

[3] C. Hofbauer, M. Huemer, and J. Huber, "Coded OFDM by unique word prefix," in *Communication Systems (ICCS), 2010 IEEE International Conference on*, Nov 2010, pp. 426–430.

[4] M. Huemer, C. Hofbauer, and J. Huber, "Non-Systematic Complex Number RS Coded OFDM by Unique Word Prefix," *Signal Processing, IEEE Transactions on*, vol. 60, no. 1, pp. 285–299, Jan 2012.

[5] A. Onic and M. Huemer, "Sphere Decoding for Unique Word OFDM," in *Global Telecommunications Conference (GLOBECOM 2011), 2011 IEEE*, Dec 2011, pp. 1–5.

[6] A. Onic, "Receiver Concepts for Unique Word OFDM," November 2013, Phd Thesis. [Online]. Available: http://uwofdm.jku.at/publications

[7] A. Chockalingam, "Low-complexity algorithms for large-MIMO detection," in *Communications, Control and Signal Processing (ISCCSP), 2010 4th International Symposium on*, March 2010, pp. 1–6.

[8] S. Mohammed, A. Chockalingam, and B. Sundar Rajan, "A Low-complexity near-ML performance achieving algorithm for large MIMO detection," in *Information Theory, 2008. ISIT 2008. IEEE International Symposium on*, July 2008, pp. 2012–2016.

[9] C. Michalke, E. Zimmermann, and G. Fettweis, "Linear Mimo Receivers vs. Tree Search Detection: A Performance Comparison Overview," in *Personal, Indoor and Mobile Radio Communications, 2006 IEEE 17th International Symposium on*, Sept 2006, pp. 1–7.

[10] S. M. Kay, *Fundamentals of Statistical Signal Processing: Estimation Theory*. Upper Saddle River, NJ, USA: Prentice-Hall, Inc., 1993.

[11] W. Koch and A. Baier, "Optimum and sub-optimum detection of coded data disturbed by time-varying intersymbol interference," in *Global Telecommunications Conference, 1990, and Exhibition. 'Communications: Connecting the Future', GLOBECOM '90., IEEE*, Dec 1990, pp. 1679–1684 vol.3.

[12] I. Collings, M. Butler, and M. McKay, "Low complexity receiver design for MIMO bit-interleaved coded modulation," in *Spread Spectrum Techniques and Applications, 2004 IEEE Eighth International Symposium on*, Aug 2004, pp. 12–16.

[13] A. Onic, A. Schenk, M. Huemer, and J. Huber, "Soft-output Sphere detection for coded Unique Word OFDM," in *Signals, Systems and Computers (ASILOMAR), 2012 Conference Record of the Forty Sixth Asilomar Conference on*, Nov 2012, pp. 138–142.

[14] A. Burg, M. Borgmann, M. Wenk, M. Zellweger, W. Fichtner, and H. Bolcskei, "VLSI implementation of MIMO detection using the sphere decoding algorithm," *Solid-State Circuits, IEEE Journal of*, vol. 40, no. 7, pp. 1566–1577, July 2005.

[15] C. Studer and H. Bolcskei, "Soft Input Soft Output Single Tree-Search Sphere Decoding," *Information Theory, IEEE Transactions on*, vol. 56, no. 10, pp. 4827–4842, Oct 2010.

[16] P. Li and R. Murch, "Multiple output selection-LAS algorithm in large MIMO systems," *Communications Letters, IEEE*, vol. 14, no. 5, pp. 399–401, May 2010.

[17] A. Chockalingam and B. S. Rajan, *Large MIMO Systems*. Cambridge University Press, 2014, cambridge Books Online. [Online]. Available: http://dx.doi.org/10.1017/CBO9781139208437

[18] S. Lin and D. J. Costello, *Error Control Coding, Second Edition*. Upper Saddle River, NJ, USA: Prentice-Hall, Inc., 2004.

[19] IEEE P802.11 Wireless LANs, *TGn Channel Models*, IEEE 802.11-03/940r4, May 2004.